

The 3-state Potts antiferromagnet on the hexagonal lattice

This article has been downloaded from IOPscience. Please scroll down to see the full text article.

1998 J. Phys. A: Math. Gen. 31 5969

(<http://iopscience.iop.org/0305-4470/31/28/011>)

View [the table of contents for this issue](#), or go to the [journal homepage](#) for more

Download details:

IP Address: 171.66.16.122

The article was downloaded on 02/06/2010 at 06:57

Please note that [terms and conditions apply](#).

The 3-state Potts antiferromagnet on the hexagonal lattice

Jesús Salas†

Departamento de Física de la Materia Condensada and Departamento de Física Teórica, Facultad de Ciencias, Universidad de Zaragoza, 50009 Zaragoza, Spain

Received 16 February 1998

Abstract. We study the 3-state hexagonal-lattice Potts antiferromagnet by a Monte Carlo simulation using the Wang–Swendsen–Kotecký cluster algorithm. We study the staggered susceptibility and the correlation length, and we confirm that this model is disordered at all temperatures $T \geq 0$. We also measure the ground-state entropy density.

1. Introduction

Antiferromagnetic Potts models [1–3] are much less well understood than their ferromagnetic counterparts. One reason for this is that the behaviour depends strongly on the microscopic lattice structure, in contrast to the universality typically enjoyed by ferromagnets. As a result, many basic questions have to be investigated case-by-case: is there a phase transition at finite temperature, and if so, of what order? What is the nature of the low-temperature phase? If there is a critical point, what are the critical exponents and the universality classes? Can these exponents be understood (for two-dimensional models) in terms of conformal field theory?

The large- q behaviour of the antiferromagnetic q -state Potts model is known rigorously [4, 5]: for q large enough (how large depends on the lattice in question), this model has a unique infinite-volume Gibbs measure and exponential decay of correlations at all temperatures, *including zero temperature*: the system is disordered as a result of the large ground-state entropy. However, for smaller values of q , phase transitions can and do occur. One expects that for each lattice \mathcal{L} there will be a value $q_c(\mathcal{L})$ such that:

- (a) for $q > q_c(\mathcal{L})$ the model has exponential decay of correlations uniformly at all temperatures, including zero temperature;
- (b) for $q = q_c(\mathcal{L})$ the model has a critical point at zero temperature;
- (c) for $q < q_c(\mathcal{L})$ any behaviour is possible. Often (though not always) the model has a phase transition at nonzero temperature, which may be of either first or second order.

The problem, for each lattice, is to find $q_c(\mathcal{L})$ and to determine the precise behaviour for each $q \leq q_c(\mathcal{L})$.

The q -state Potts model on a lattice \mathcal{L} is defined by the Hamiltonian

$$\mathcal{H} = -J \sum_{\langle xy \rangle} \delta_{\sigma_x, \sigma_y} \quad (1.1)$$

where the sum $\sum_{\langle xy \rangle}$ runs over all possible nearest-neighbour pairs of lattice sites (each pair counted once), and each spin takes values $\sigma_x \in \{1, \dots, q\}$. The antiferromagnetic case

† E-mail address: jesus@jupiter.unizar.es

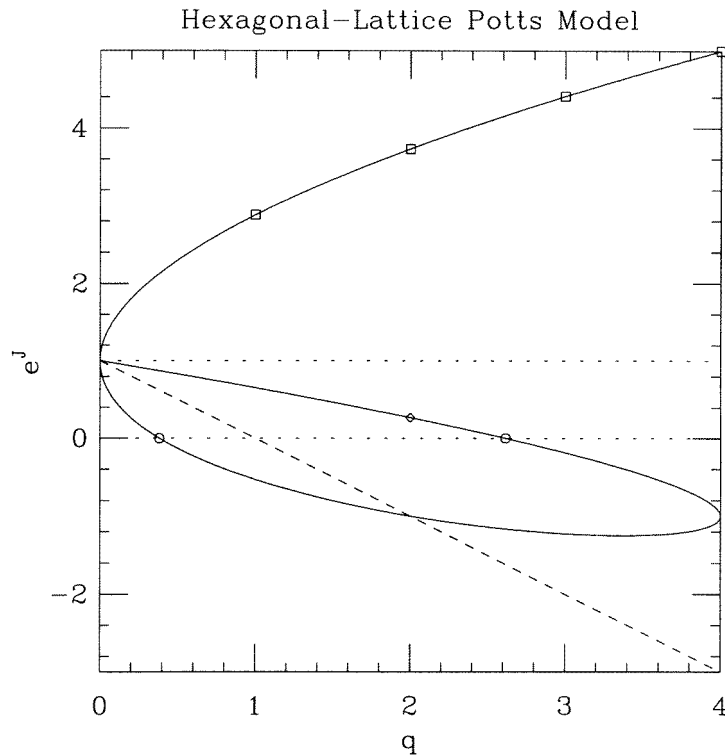


Figure 1. Curves where the hexagonal-lattice Potts model has been solved: $(e^J - 1)^3 - 3q(e^J - 1) = q^2$ (full curve), which has three branches; and the line $e^J = 1 - q$ (broken line). The horizontal dotted lines correspond to $e^J = 1$ (separating the ferromagnetic and antiferromagnetic regimes) and to $e^J = 0$ (separating the antiferromagnetic regime from the unphysical region $e^J < 0$). The squares show the known ferromagnetic critical points ($q = 1, 2, 3, 4$); and the diamond marks the known antiferromagnetic critical point for $q = 2$. The open circles show the points where the two antiferromagnetic branches cross the $e^J = 0$ line, namely $q = (3 \pm \sqrt{5})/2$.

corresponds to $J = -\beta < 0$. The Potts antiferromagnet on the hexagonal (honeycomb) lattice is the simplest case. First, we know that the $q = 2$ model has a critical point at $e^J = 2 - \sqrt{3}$ because the corresponding ferromagnetic model is critical at $e^J = 2 + \sqrt{3}$, and the hexagonal lattice is bipartite. Second, the results of [5] show that the hexagonal-lattice antiferromagnet exhibits exponential decay of correlations at zero temperature for $q \geq 4$. Thus, $q_c(hc)$ should lie somewhere strictly between $q = 2$ and $q = 4$. The behaviour at $q = 3$ has not yet been analysed rigorously.

On the other hand, the q -state hexagonal-lattice Potts model has been solved (e.g. the free and internal energies are exactly known) on two special curves in the (J, q) plane (see figure 1):

$$(e^J - 1)^3 - 3q(e^J - 1) = q^2 \quad (1.2)$$

$$e^J = 1 - q \quad \text{for } 0 < q < 4. \quad (1.3)$$

These curves are the duality images [6] of the corresponding curves for the triangular-lattice Potts antiferromagnet obtained by Baxter and collaborators [7–9]. Curve (1.2) has three branches in the region $q \geq 0$; the uppermost branch (with $0 \leq q \leq \infty$ and $e^J \geq 1$) corresponds to the ferromagnetic critical line; the middle branch (with $0 \leq q \leq 4$ and

$-1 \leq e^J \leq 1$) contains the $q = 2$ antiferromagnetic critical point ($e^J = 2 - \sqrt{3}$) and crosses the zero-temperature line $e^J = 0$ at $q = (3 + \sqrt{5})/2 \approx 2.618$; the lowermost branch crosses the zero-temperature line at $q = (3 - \sqrt{5})/2 \approx 0.382$ [†]. The second curve (1.3) is physical ($e^J \geq 0$) only for $0 \leq q \leq 1$.

The behaviour of the middle branch suggests that it may be the antiferromagnetic critical curve. If this is the case, there would be a zero-temperature critical point at

$$q = q_c(hc) = \frac{3 + \sqrt{5}}{2} \quad (1.4)$$

(if this assertion has any meaning[‡]) and the model would be disordered at all temperatures for $q > q_c(hc)$. This conclusion is in agreement with the exact result of [5]. Further interesting speculations can be found in [10].

Shrock and Tsai [15] used this theoretical argument to rule out the existence of a critical point in the 3-state antiferromagnet. They also pointed out that this argument could fail if there was a first-order phase transition (with finite correlation length). To test these ideas, they performed Monte Carlo simulations over a large range of temperatures ($0 \leq \beta \leq 5$), and studied the (static and dynamic) behaviour of the energy density. They found no signal of hysteresis, and no critical slowing-down at large β for the Metropolis [16] and Swendsen–Wang cluster [17, 18] algorithms. They finally concluded that the model is disordered at all temperatures $T \geq 0$.

However, the numerical results of [15] (namely, smoothness of the energy density and boundedness of its integrated autocorrelation time for Metropolis and Swendsen–Wang algorithms) do not constitute *strong* evidence supporting the absence of criticality of this model. A closely related model (e.g. the 3-state square-lattice Potts antiferromagnet [6, 19]) makes an excellent counterexample: it has a critical point at $T = 0$, but the energy density is smooth over the entire temperature range, and the autocorrelation times for the Wang–Swendsen–Kotecký (WSK) cluster algorithm [20, 21] are uniformly bounded $\tau_{\text{int}} \lesssim 7.6$ [22–24]. On the other hand, the absence of critical slowing-down at large β for the (local) Metropolis algorithm only implies that the specific heat C_H is bounded. This comes from the rigorous bound [25]:

$$\tau_{\text{int}, \mathcal{E}} \gtrsim V C_H \quad (1.5)$$

where V is the volume. Thus, a direct test of non-criticality for the 3-state hexagonal-lattice Potts antiferromagnet is still lacking. This test can be achieved, for instance, by measuring the staggered susceptibility and the correlation length.

Finally, the above-mentioned argument, which identifies exact solubility with criticality, though plausible, is not necessarily valid. For example, in the triangular-lattice case there are two curves where the model can be solved, and the antiferromagnetic critical point of the $q = 2$ model (namely, $e^J = 0$) happens to lie on both of these curves. Moreover, the

[†] The middle branch is missing in [10, p 673, figure 8].

[‡] The Potts models for noninteger q can be given a rigorous meaning via the mapping onto the Fortuin–Kasteleyn random-cluster model [11–13]. The trouble is that in the antiferromagnetic case ($J < 0$) this latter model has negative weights, and so cannot be given a standard probabilistic interpretation. In particular, the existence of a good infinite-volume limit is problematical; the limit could depend strongly on the subsequence of lattice sizes and on the boundary conditions. The same is true of the ‘anti-Fortuin–Kasteleyn’ representation, in which the coefficients are products of chromatic polynomials of clusters: again the weights can be negative for noninteger q , and the existence of the infinite-volume limit is problematical. Likewise, the ice-model representation [6, 14] has in general complex weights for $0 < q < 4$, even in the ferromagnetic case.

antiferromagnetic critical point of the $q = 4$ model, which is believed [8, 26–28]† to be at $e^J = 0$, lies on *one* (though not the other) of these curves. Nevertheless, *neither* of these two curves can properly be identified with the antiferromagnetic critical curve of this model, as this identification would predict an incorrect scenario for $q = 3$ (see [5] for details).

In this note, we report the results of performing a direct test of noncriticality and we show with no ambiguities that the 3-state Potts antiferromagnet on the hexagonal lattice is always disordered. In section 2 we describe the method we have used to simulate the system and the operators we have measured. In section 3 we display the results for the energy, specific heat, staggered susceptibility and second-moment correlation length. All these quantities (as well as the corresponding integrated autocorrelation times) are bounded *uniformly* in the temperature and the lattice size. We conclude that the 3-state hexagonal-lattice Potts antiferromagnet is disordered at all temperatures $T \geq 0$. As a by-product of our calculation, we compute the zero-temperature entropy density.

2. Numerical simulations

We have performed Monte Carlo simulations of the 3-state hexagonal-lattice Potts antiferromagnet at temperatures ranging from $T = \infty$ to $T = 0$. More precisely, we have simulated this model from $\beta = 0$ to $\beta = 9$ in intervals of 0.05, and also exactly at $\beta = \infty$. We have made our simulations using the WSK cluster algorithm. This algorithm is quite simple: choose randomly two distinct states $\mu, \nu \in \{1, \dots, q\}$; freeze all the spins taking values $\neq \mu, \nu$, and allow the remaining spins to take the value either μ or ν . The induced antiferromagnetic Ising model is then simulated using the standard Swendsen–Wang algorithm [17, 18]: form bonds between nearest-neighbour sites taking distinct spin values (i.e. one taking the value μ and the other one, ν) with probability $p = 1 - e^{-\beta}$; identify the clusters of sites connected by bonds, and for each cluster either keep the original configuration or flip it (i.e. $\mu \leftrightarrow \nu$) with equal probability. The WSK algorithm is suitable to simulate this model *at zero temperature* because our lattices are bipartite [29, 24]. At $\beta = 0$ we have started the simulations with a random configuration; at finite $\beta > 0$, we started from the last configuration generated at the closest smallest β ; and at $\beta = \infty$ we started from an ordered configuration (spins in one sublattice all equal to 1, and spins on the other sublattice all equal to 2).

The hexagonal lattice is not a Bravais lattice [30], as not all points are equivalent. Rather, it is the union of two sublattices, the even and odd, each of which is isomorphic to a triangular lattice (whose lattice spacing is larger by a factor of $\sqrt{3}$). The hexagonal lattice can thus be viewed as an underlying triangular lattice (which *is* Bravais) with a two-point basis. To be more precise, consider a finite hexagonal lattice \mathcal{H} with periodic boundary conditions. Then the even sublattice of \mathcal{H} is a triangular lattice \mathcal{T} . Conversely, given an $L \times L$ triangular lattice \mathcal{T} with periodic boundary conditions, we can construct a hexagonal lattice \mathcal{H} with $V_{hc} = 2L^2$ points by taking the sites in \mathcal{T} together with the centres of the down-pointing elementary triangles of \mathcal{T} . Thus, a generic point \mathbf{x} of the hexagonal lattice can be written as [31]:

$$\mathbf{x} = x'_1 \boldsymbol{\eta}_1 + x'_2 \boldsymbol{\eta}_2 + \boldsymbol{\epsilon} \boldsymbol{\eta} \equiv \mathbf{x}' + \boldsymbol{\epsilon} \boldsymbol{\eta} \quad (2.1a)$$

$$x'_1, x'_2 = 1, \dots, L \quad (2.1b)$$

† The authors of [27] studied the 3-colouring model on the hexagonal lattice, which is equivalent to the 3-state Potts antiferromagnet on the Kagomé lattice *at zero temperature*. This latter model can be exactly mapped onto the 4-state Potts antiferromagnet on the triangular lattice *at zero temperature* [28].

where \mathbf{x}' lives on the triangular lattice spanned by the (unit) vectors

$$\boldsymbol{\eta}_1 = (1, 0) \tag{2.2a}$$

$$\boldsymbol{\eta}_2 = \left(-\frac{1}{2}, \frac{\sqrt{3}}{2}\right) \tag{2.2b}$$

and L is the linear size of the triangular sublattices[†]. In this paper we have considered lattices ranging from $L = 3$ to $L = 48$. The variable $\epsilon = 0, 1$ can be interpreted as the ‘parity’ of the corresponding lattice site: if $\epsilon = 0$ (resp. $\epsilon = 1$) the site \mathbf{x} belongs to the even (resp. odd) sublattice. The vector

$$\boldsymbol{\eta} = \frac{1}{\sqrt{3}}(0, 1) = \frac{1}{3}(\boldsymbol{\eta}_1 + 2\boldsymbol{\eta}_2) \tag{2.3}$$

is the so-called basis vector joining the two points of the basis. The pair (\mathbf{x}', ϵ) determines uniquely a point on the hexagonal lattice, and conversely, given a point \mathbf{x} of the hexagonal lattice we can uniquely obtain the pair (\mathbf{x}', ϵ) associated to it.

We have measured three basic observables. The simplest one is the energy

$$\mathcal{E} = \sum_{\langle xy \rangle} \delta_{\sigma_x \sigma_y}. \tag{2.4}$$

The staggered magnetization can be written easily if we represent the spin at site \mathbf{x} by a vector in the plane

$$\boldsymbol{\sigma}_x = \left(\cos \frac{2\pi}{3} \sigma_x, \sin \frac{2\pi}{3} \sigma_x\right). \tag{2.5}$$

In this case, the staggering assigns a phase $e^{i\pi\epsilon} = (-1)^\epsilon$ depending solely on which sublattice the spin is located[‡]. The square of the staggered magnetization can be written as

$$\mathcal{M}_{\text{stagg}}^2 = \left(\sum_{\mathbf{x}', \epsilon} (-1)^\epsilon \boldsymbol{\sigma}_{\mathbf{x}'+\epsilon\boldsymbol{\eta}}\right)^2 = \frac{3}{2} \sum_{\alpha=1}^3 \left| \sum_{\mathbf{x}', \epsilon} (-1)^\epsilon \delta_{\sigma_{\mathbf{x}'+\epsilon\boldsymbol{\eta}}, \alpha} \right|^2. \tag{2.6}$$

This is a ‘zero-momentum’ observable. In order to estimate the second-moment correlation length we have to define the corresponding ‘smallest-nonzero-momentum’ observable. The translational invariance of the hexagonal lattice \mathcal{H} is given by the underlying triangular (Bravais) lattice \mathcal{T} . Thus, the allowed momenta are those of a triangular lattice of size $L \times L$ with periodic boundary conditions [30]:

$$\mathbf{k} = \frac{2\pi}{L} m_1 \boldsymbol{\rho}_1 + \frac{2\pi}{L} m_2 \boldsymbol{\rho}_2 \tag{2.7a}$$

$$m_1, m_2 = 1, \dots, L. \tag{2.7b}$$

[†] We have chosen the lattice spacing of the triangular sublattice to be $a_{\mathcal{T}} = 1$; the lattice spacing of the corresponding hexagonal lattice is therefore $a_{\mathcal{H}} = 1/\sqrt{3}$.

[‡] This choice is motivated by what happens in the $q = 2$ case: at $T = 0$ all the spins on the even sublattice take one value (say, 1), and all the spins on the other sublattice take the other value (say, 2). The natural staggering corresponds to assign a phase $e^{i\pi}$ to all the spins on the odd sublattice. We can generalize this to the $q = 3$ case by assigning a general phase $e^{i\phi}$ to all the spins on the odd sublattice. Then, the contribution of the six smallest momenta (2.10) to the observable (2.11) is the same in average only when $\phi = 0$ (uniform magnetization), and $\phi = \pi$ (staggered magnetization).

The momenta are given in the basis

$$\rho_1 = \frac{2}{\sqrt{3}} \left(\frac{\sqrt{3}}{2}, \frac{1}{2} \right) \tag{2.8a}$$

$$\rho_2 = \frac{2}{\sqrt{3}} (0, 1) \tag{2.8b}$$

defined by the relations

$$\eta_i \cdot \rho_j = \delta_{ij}. \tag{2.9}$$

The smallest nonzero momenta are

$$\mathbf{k} = \left\{ \pm \frac{2\pi}{L} \rho_1, \pm \frac{2\pi}{L} \rho_2, \pm \frac{2\pi}{L} (\rho_1 - \rho_2) \right\} \tag{2.10}$$

all having $|\mathbf{k}| = 4\pi/(\sqrt{3}L)$. Thus, the smallest-nonzero-momentum observable associated to (2.6) is

$$\mathcal{F}_{\text{stagg}} = \frac{3}{2} \times \frac{1}{6} \sum_{n=1}^6 \sum_{\alpha=1}^3 \left| \sum_{x', \epsilon} (-1)^\epsilon e^{i\mathbf{k}_n \cdot (x' + \epsilon \eta)} \delta_{\sigma_{x' + \epsilon \eta}, \alpha} \right|^2. \tag{2.11}$$

The contributions of the wavevectors \mathbf{k}_n and $-\mathbf{k}_n$ are exactly the same; thus equation (2.11) can be simplified:

$$\begin{aligned} \mathcal{F}_{\text{stagg}} = \frac{3}{2} \times \frac{1}{3} \sum_{\alpha=1}^3 \left\{ \left| \sum_{x'} e^{2\pi i x'_1/L} [\delta_{\sigma_{x'}, \alpha} - e^{2\pi i/3L} \delta_{\sigma_{x'+\eta}, \alpha}] \right|^2 \right. \\ \left. + \left| \sum_{x'} e^{2\pi i x'_2/L} [\delta_{\sigma_{x'}, \alpha} - e^{4\pi i/3L} \delta_{\sigma_{x'+\eta}, \alpha}] \right|^2 \right. \\ \left. + \left| \sum_{x'} e^{2\pi i (x'_1 - x'_2)/L} [\delta_{\sigma_{x'}, \alpha} - e^{-2\pi i/3L} \delta_{\sigma_{x'+\eta}, \alpha}] \right|^2 \right\}. \end{aligned} \tag{2.12}$$

From these observables we have computed the following expectation values: the energy density (per spin)

$$E = \frac{1}{V_{hc}} \langle \mathcal{E} \rangle \tag{2.13}$$

the specific heat

$$C_H = \frac{1}{V_{hc}} \text{var}(\mathcal{E}) \equiv \frac{1}{V_{hc}} [\langle \mathcal{E}^2 \rangle - \langle \mathcal{E} \rangle^2] \tag{2.14}$$

the staggered susceptibility

$$\chi_{\text{stagg}} = \frac{1}{V_{hc}} \langle \mathcal{M}_{\text{stagg}}^2 \rangle \tag{2.15}$$

and the second-moment correlation length

$$\xi = \frac{(\chi_{\text{stagg}}/F_{\text{stagg}} - 1)^{1/2}}{2 \sin(\pi/L)} \tag{2.16}$$

where F_{stagg} is given by

$$F_{\text{stagg}} = \frac{1}{V_{hc}} \langle \mathcal{F}_{\text{stagg}} \rangle. \quad (2.17)$$

For each observable \mathcal{O} discussed above we have measured its integrated autocorrelation time $\tau_{\text{int},\mathcal{O}}$ using a self-consistent truncation window of width $6\tau_{\text{int}}$ [32, appendix C].

We have made 5×10^5 (resp. 3.5×10^5) iterations for $L = 3, 6$ (resp. $L \geq 9$). We have discarded 10% of them to allow the system to reach equilibrium. The autocorrelation times for all the observables were uniformly bounded in β and L :

$$\tau_{\text{int}} \lesssim 4. \quad (2.18)$$

For $L \geq 9$ there is a sharper bound: $\tau_{\text{int}} \lesssim 3^\dagger$. This means that we have made $\approx 10^5 \tau_{\text{int}}$ measurements, and we have discarded $\approx 10^4 \tau_{\text{int}}$ iterations as a (conservative) prevention against the existence of any slower mode not considered here.

We have made our simulations on two Pentium machines at 166 MHz. Each WSK iteration took approximately $3 \times (2L^2) \mu\text{s}$; the total CPU used was approximately 13 days.

3. Data analysis

In this section we perform all fits using the standard weighted least-squares method. As a precaution against corrections to scaling, we impose a lower cut-off $L \geq L_{\text{min}}$ on the data points admitted in the fit, and we study systematically the effects of varying L_{min} on both the estimated parameters and the χ^2 . In general, our preferred fit corresponds to the smallest L_{min} for which the goodness of fit is reasonable (e.g. the confidence level ‡ is $\gtrsim 10$ –20%) and for which subsequent increases in L_{min} do not cause the χ^2 to drop vastly more than one unit per degree of freedom (DF).

Let us first consider the second-moment correlation length $\xi = \xi(\beta, L)$ (see figure 2). We see that this observable is, for fixed L , a nondecreasing function of β which asymptotically tends to the value at $\beta = \infty$ (i.e. $\xi(\beta = \infty, L)$). At fixed β , the function $\xi(\beta, \cdot)$ is also nondecreasing. For $L \geq 12$, the values of $\xi(\beta, L)$ collapses well onto a single curve. Furthermore, $\xi(\beta, L) \lesssim 3.2$ uniformly in β and L . Thus, the correlation length stays bounded even at $T = 0$; this observation implies that there is no critical point for this model at any temperature $T \geq 0$ § .

If we fit the values of $\xi(\infty, L)$ to a constant ($=\xi(\infty, \infty)$) we obtain a good fit for $L_{\text{min}} = 12$,

$$\xi(\infty, \infty) = 3.0828 \pm 0.0098 \quad (3.1)$$

with $\chi^2 = 1.61$ (2 DF, level = 45%). Thus, $\xi(\beta, L) \leq \xi(\infty, \infty)$ uniformly in β and L . The numerical value of $\xi(\infty, \infty)$ is consistent with the observation that the thermodynamic limit is attained in practice (i.e. $\xi(\beta, L) \ll L$) for $L \geq 12$. Therefore, we do not have to consider larger lattices (i.e. $L > 48$).

† The fact that τ_{int} is larger for smaller lattices can be understood because the correlation length satisfies $\xi \lesssim 3$ for all T and L . For small L , the ratio ξ/L is not much smaller than 1; however, for large L , $\xi/L \ll 1$.

‡ The ‘confidence level’ is the probability that χ^2 would exceed the observed value, assuming that the underlying statistical model is correct. An unusually low confidence level (e.g. less than 5%) thus suggests that the underlying statistical model is *incorrect*—the most likely cause of which would be corrections to scaling.

§ In figure 2 we observe that the error bars for $L = 24$ are noticeably larger than the rest, especially in the high-temperature (or small correlation length) region. This feature is solely a consequence of the definition of the second-moment correlation length (2.16). It is easy to see that its error bar behaves like $\sigma(\xi) \sim L^2/\xi$ when $L \gg 1$. This feature is absent in the other observables we have considered here (see figure 3).

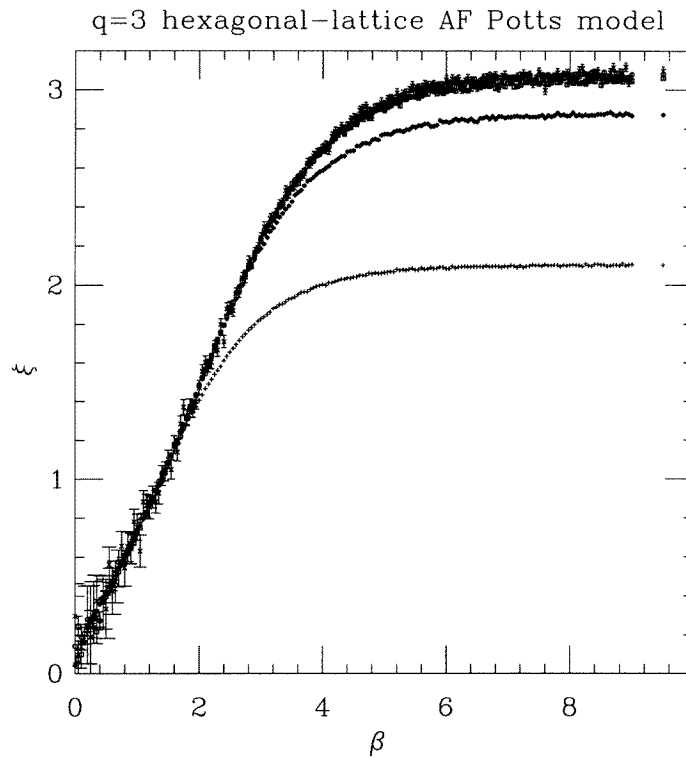


Figure 2. Second-moment correlation length ξ of the 3-state hexagonal-lattice Potts antiferromagnet as a function of β and L . Symbols indicate $L = 3$ (+), $L = 6$ (\diamond), $L = 9$ (\square), $L = 12$ (\circ), and $L = 24$ (\times). Points with $L = 48$ coincide with $L = 24$, and they are not shown for clarity. The isolated points on the far right of the picture (displayed for convenience at $\beta = 9.5$) are the data from the runs at $\beta = \infty$.

This scenario also applies to the staggered susceptibility (see figure 3). This observable $[\chi_{\text{stagg}}(\beta, L)]$ is also a nondecreasing function of β at fixed L , and of L at fixed β . Moreover, for $L \geq 12$ the measurements collapse well onto a single curve, which is uniformly bounded: $\chi_{\text{stagg}}(\beta, L) \lesssim 20$. There is no signal of second-order or first-order phase transition at any temperature.

If we fit the value of the staggered susceptibility at zero temperature $\chi_{\text{stagg}}(\beta = \infty, L)$ to a constant ($= \chi_{\text{stagg}}(\infty, \infty)$), we obtain a good fit for $L_{\text{min}} = 24$

$$\chi_{\text{stagg}}(\infty, \infty) = 19.070 \pm 0.043 \quad (3.2)$$

with $\chi^2 = 0.48$ (1 DF, level = 49%).

The energy and specific heat are both nonincreasing curves which tend asymptotically to zero as $\beta \rightarrow \infty$. For $L \geq 6$ the points fall very approximately onto a single curve; for both observables the finite-size corrections are very small. Our curve for the energy coincides with that of Shrock and Tsai [15]. The specific heat does not show any signal of transition points: it also decays smoothly to zero as $\beta \rightarrow \infty$.

In conclusion, there is no signal of phase transitions at any temperature $T \geq 0$ in the 3-state hexagonal-lattice Potts antiferromagnet. This model is disordered at all temperatures.

From the energy density one can easily compute the entropy density (per spin) of this

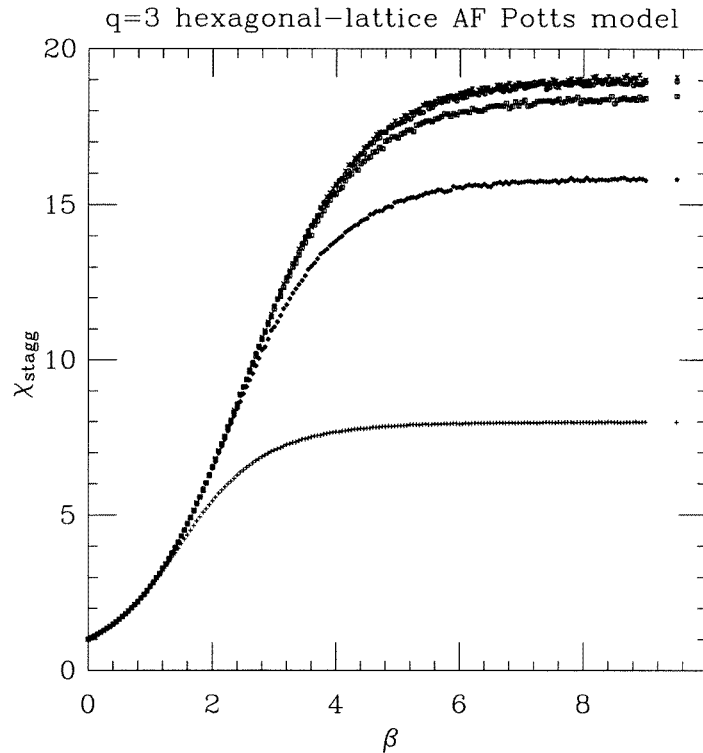


Figure 3. Staggered susceptibility χ_{stagg} of the 3-state hexagonal-lattice Potts antiferromagnet as a function of β and L . Symbols are as in figure 2.

model [33]:

$$S(\beta) \equiv S(0) + \beta E(\beta) - \int_0^\beta E(\beta') d\beta' \tag{3.3}$$

where the value of the entropy at $\beta = 0$ is given by $S_{hc,q=3}(\beta = 0) = \log q = \log 3$.

Using our numerical data, we are able to compute the value of the entropy at $\beta = 9$, and we have to extrapolate this value somehow to $\beta = \infty$. One way to achieve this is the following. At very large β we are deep in the strong coupling limit, so we expect that the energy density behaves as $E(\beta) \sim Ae^{-\beta} + \mathcal{O}(e^{-2\beta})$ †. If this is the case, we can compute exactly the integral on the r.h.s. of (3.3) and relate the result to the energy density at β :

$$S(\infty) = S(0) - E(\beta) - \int_0^\beta E(\beta') d\beta'. \tag{3.4}$$

Now the maximum value of β where we have computed the energy becomes a cut-off. For each lattice size L , we have computed the values of $S(\beta = \infty, L)$ with this method using different values of the cut-off β ; the results were consistent within statistical errors

† Although there is no obvious way to perform low-temperature series expansion for this model—there are too many inequivalent ground states—it is reasonable to expect that there is an expansion in powers of $e^{-\beta}$, which corresponds to the minimum energy cost for a ‘overturned’ spin. Indeed, our numerical data behaves in this way for large enough β .

(usually the differences were much smaller than the statistical errors). The values of the entropy density at zero temperature are displayed in table 1. The error bars are the sum of the statistical errors (coming from the statistical errors of the energies) and the systematic errors coming from the integration algorithm. We have used several extended trapezoidal rules and different sizes of the integration intervals [34]: the systematic error takes account (conservatively) of the differences we found.

Table 1. Values of the 3-state hexagonal-lattice Potts antiferromagnet entropy density at zero temperature $S_{hc,3}(\beta = \infty, L)$ as a function of the lattice size L . The error bars are the sum of the statistical and systematic errors

L	$S_{hc,3}(\infty, L)$
3	$0.535\,387 \pm 0.000\,158$
6	$0.509\,207 \pm 0.000\,097$
9	$0.507\,220 \pm 0.000\,089$
12	$0.506\,952 \pm 0.000\,043$
24	$0.506\,864 \pm 0.000\,062$
48	$0.506\,843 \pm 0.000\,012$

If we fit the data to a constant ($= S_{hc,3}(\infty, \infty)$) we find a good fit only for $L_{\min} = 24$

$$S_{hc,3}(\infty, \infty) = 0.506\,844 \pm 0.000\,012 \quad (3.5)$$

with $\chi^2 = 0.11$ (1 DF, level = 74%). This number is in agreement with Shrock and Tsai [15, 35]:

$$S_{hc,3}(\infty, \infty)_{\text{ST}} = 0.5068 \pm 0.0003 \quad (3.6)$$

but the error bar is one order of magnitude smaller than in [35]. If we use the extended ansatz of [35],

$$S_{hc,3}(\beta = \infty, L) = S_{hc,3}(\infty, \infty) + \frac{c_1}{L^2} + \frac{c_2}{L^4} + \frac{c_3}{L^6} \quad (3.7)$$

we can reasonably fit all data (i.e. $L_{\min} = 3$) giving

$$S_{hc,3}(\infty, \infty) = 0.506\,841 \pm 0.000\,018 \quad (3.8)$$

with $\chi^2 = 0.40$ (2 DF, level = 82%). This estimator agrees within errors with (3.5)/(3.6)†.

Indeed, the estimator (3.8) is contained within the rigorous lower and upper bounds obtained by Shrock and Tsai for the hexagonal lattice [36, 37]:

$$\frac{(q^4 - 5q^3 + 10q^2 - 10q + 5)^{1/2}}{q - 1} \leq e^{S_{hc,q}(\infty, \infty)} \leq (q^2 - 3q + 3)^{1/2}. \quad (3.9)$$

For $q = 3$ these bounds become

$$0.505\,800\dots = \log\left(\frac{\sqrt{11}}{2}\right) \leq S_{hc,3}(\infty, \infty) \leq \log(\sqrt{3}) = 0.549\,306\dots \quad (3.10)$$

† An ansatz of the form $S_{hc,3}(\beta = \infty, L) = S_{hc,3}(\infty, \infty) + c_1/L^2$ is unable to fit well the data for any value of L_{\min} . If we add a term c_2/L^4 , we get a good fit for $L_{\min} = 6$, giving $S_{hc,3}(\infty, \infty) = 0.506\,847 \pm 0.000\,013$ with $\chi^2 = 0.075$ (1 DF, level = 78%). The ansatz (3.7) is the first one to be able to fit all the data ($L_{\min} = 3$). Adding a term c_4/L^8 does not modify the conclusions.

The lower bound is remarkably sharp: in [37] it is shown that if we extract the leading term $[= q(1 - 1/q)^{3/2}]$ and expand the rest in powers of $y = 1/(q - 1)$, the resulting series for $e^{S_{hc,q}(\infty,\infty)}$ and its rigorous lower bound (cf (3.9)) agree up to $\mathcal{O}(y^{10})$. The lower bound gives a very good approximation even for q as low as $q = 3$.

The zero-temperature entropy density (3.8) is a large fraction ($\approx 46\%$) of the entropy at $T = \infty$ [$S_{hc,3}(\beta = 0) = \log 3 = 1.098\,61\dots$]. This large ground-state entropy makes the system disordered at zero temperature.

Acknowledgments

We wish to thank Alan Sokal for encouragement and illuminating discussions, Robert Shrock for correspondence and Chris Henley for making available some of his unpublished notes. The author's research was supported in part by CICyT grants PB95-0797 and AEN97-1680.

References

- [1] Potts R B 1952 *Proc. Camb. Phil. Soc.* **48** 106
- [2] Wu F Y 1982 *Rev. Mod. Phys.* **54** 235
Wu F Y 1983 *Rev. Mod. Phys.* **55** 315 (erratum)
- [3] Wu F Y 1984 *J. Appl. Phys.* **55** 2421
- [4] Kotecký R cited in Georgii H-O 1988 *Gibbs Measures and Phase Transitions* (Berlin: de Gruyter) pp 148–9, 457
- [5] Salas J and Sokal A D 1997 *J. Stat. Phys.* **86** 551
- [6] Baxter R J 1982 *Exactly Solved Models in Statistical Mechanics* (New York: Academic)
- [7] Baxter R J, Temperley H N V and Ashley S E 1978 *Proc. R. Soc. A* **358** 535
- [8] Baxter R J 1986 *J. Phys. A: Math. Gen.* **19** 2821
- [9] Baxter R J 1987 *J. Phys. A: Math. Gen.* **20** 5241
- [10] Saleur H 1990 *Commun. Math. Phys.* **132** 657
- [11] Kasteleyn P W and Fortuin C M 1969 *J. Phys. Soc. Japan Suppl.* **26** 11
- [12] Fortuin C M and Kasteleyn P W 1972 *Physica* **57** 536
- [13] Fortuin C M 1972 *Physica* **58** 393
Fortuin C M 1972 *Physica* **59** 545
- [14] Baxter R J, Kelland S B and Wu F Y 1976 *J. Phys. A: Math. Gen.* **9** 397
- [15] Shrock R and Tsai S-H 1997 *J. Phys. A: Math. Gen.* **30** 495
- [16] Metropolis N, Rosenbluth A W, Rosenbluth M N, Teller A H and Teller E 1953 *J. Chem. Phys.* **21** 1087
- [17] Swendsen R H and Wang J-S 1987 *Phys. Rev. Lett.* **58** 86
- [18] Wang J-S and Swendsen R H 1990 *Physica* **167A** 565
- [19] Baxter R J 1982 *Proc. R. Soc. A* **383** 43
- [20] Wang J-S, Swendsen R H and Kotecký R 1989 *Phys. Rev. Lett.* **63** 109
- [21] Wang J-S, Swendsen R H and Kotecký R 1990 *Phys. Rev. B* **42** 2465
- [22] Ferreira S J and Sokal A D 1995 *Phys. Rev. B* **51** 6727
- [23] Salas J and Sokal A D 1998 The 3-state square-lattice Potts antiferromagnet at zero temperature *Preprint* cond-mat/9801079 (to appear in *J. Stat. Phys.*)
- [24] Ferreira S J and Sokal A D in preparation
- [25] Caracciolo S, Pelissetto A and Sokal A D 1994 *Phys. Rev. Lett.* **72** 179
- [26] Baxter R J 1970 *J. Math. Phys.* **11** 784
- [27] Kondev J and Henley C L 1996 *Nucl. Phys. B* **52** 6628
- [28] Henley C L in preparation
- [29] Burton J K Jr and Henley C L 1998 *J. Phys. A: Math. Gen.* **30** 8385
- [30] Ashcroft N W and Mermin N D 1976 *Solid State Physics* (Philadelphia, PA: Saunders)
- [31] Campostrini M, Pelissetto A, Rossi P and Vicari E 1998 *Phys. Rev. E* **57** 184
- [32] Madras N and Sokal A D 1998 *J. Stat. Phys.* **50** 679
- [33] Binder K 1981 *Z. Phys. B* **45** 61
- [34] Press W H, Teukolsky S A, Vetterling W T and Flannery B P 1992 *Numerical Recipes in C: The Art of Scientific Computing* (Cambridge: Cambridge University Press)

- [35] Shrock R and Tsai S-H 1997 *Phys. Rev. E* **55** 5165
- [36] Shrock R and Tsai S-H 1997 *Phys. Rev. E* **55** 6791
- [37] Shrock R and Tsai S-H 1997 *Phys. Rev. E* **56** 2733